Development 130, 1725-1734

doi:10.1242/dev.00407

The left-right determinant Inversin is a component of node monocilia and other 9+0 cilia

Daisuke Watanabe[1,*], Yukio Saijoh[1,*], Shigenori Nonaka[1,*], Genta Sasaki[1,*], Yayoi Ikawa[1,*], Takahiko Yokoyama[2,†] and Hiroshi Hamada[1,*,‡]

[1]Developmental Genetics Group, Graduate School of Frontier Biosciences, Osaka University, 1-3 Yamada-oka, Suita, Osaka 565-0871, Japan
[2]Department of Anatomy and Developmental Biology, Tokyo Women's Medical University, School of Medicine, 8-1 Kawada-cho, Shinjuku-ku, Tokyo 162-8600, Japan
*CREST, Japan Science and Technology Corporation (JST)
†Present address: Department of Anatomy and Developmental Biology, Kyoto Prefecture University of Medicine, Kawaramachi-Hirokoji, Kamikyo-ku, Kyoto 602-0841, Japan
‡Author for correspondence (e-mail: hamada@fbs.osaka-u.ac.jp)

Accepted 13 January 2003

SUMMARY

Inversin (Inv), a protein that contains ankyrin repeats, plays a key role in left-right determination during mammalian embryonic development, but its precise function remains unknown. Transgenic mice expressing an Inv and green fluorescent protein (GFP) fusion construct (Inv::GFP) were established to facilitate characterization of the subcellular localization of Inv. The *Inv::GFP* transgene rescued the laterality defects and polycystic kidney disease of *Inv/Inv* mice, indicating that the fusion protein is functional. In transgenic embryos, Inv::GFP protein was detected in the node monocilia. The fusion protein was also present in other 9+0 monocilia, including those of kidney epithelial cells and the pituitary gland, but it was not localized to 9+2 cilia. The N-terminal region of Inv (InvΔC) including the ankyrin repeats also localized to the node cilia and rescued the left-right defects of *Inv/Inv* mutants. Although no obvious abnormalities were detected in the node monocilia of *Inv/Inv* embryos, the laterality defects of such embryos were corrected by an artificial leftward flow of fluid in the node, suggesting that nodal flow is impaired by the *Inv* mutation. These results suggest that the Inv protein contributes to left-right determination as a component of monocilia in the node and is essential for the generation of normal nodal flow.

Movie available online

Key words: Cilia, Inv, Left-right asymmetry, Node, Mouse

INTRODUCTION

Vertebrates exhibit numerous left-right (LR) asymmetries, such as the positions of the heart and spleen on the left side of the body (Fujinaga, 1997). The process by which LR asymmetry is established can be divided into three phases: (1) the initial determination of LR polarity; (2) LR asymmetric expression of signaling molecules; and (3) LR asymmetric morphogenesis induced by these signaling molecules (Beddington and Robertson, 1999; Capdevila et al., 2000; Wright, 2001; Yost, 2001; Hamada et al., 2002).

In spite of recent progress, our knowledge of LR determination remains limited. In particular, the mechanism by which symmetry is initially broken remains unknown, although several models have been proposed (Brown and Wolpert, 1990; Brown et al., 1991). Cilia and fluid flow have been implicated in LR determination (Nonaka et al., 1998; Okada et al., 1999). Monocilia on the node pit cells rotate in a clockwise direction and thereby generate a leftward flow of extra-embryonic fluid (referred to as nodal flow). We recently directly demonstrated a role for nodal flow in LR determination by examining the effects of artificial flow (Nonaka et al., 2002). An artificial rightward flow that was fast enough to reverse the endogenous leftward flow was thus able to reverse LR patterning in mouse embryos. Although it remains unclear how nodal flow contributes to LR determination, it is possible that the flow transports an unknown morphogen toward the left side of the embryo. Alternatively, mechanical stress induced by the flow might be sensed by cells in or near the node.

Various mouse mutants with defects in the initial determination of LR polarity have been identified. The absence of nodal flow, however, may account for the situs defects of most of these mutants. Mutant mice with impaired nodal flow can be classified into two groups: those lacking the node cilia and those with immotile node cilia. The first group includes mice deficient in the kinesin superfamily proteins KIF3A (Marszalek et al., 1999; Takeda et al., 1999) or KIF3B (Nonaka et al., 1998). Other mutants, such as those deficient in polaris (Murcia et al., 2000), probably also belong to this group. The second group includes the *Iv/Iv* mutant (Supp et al., 1997; Supp et al., 1999) and, possibly, mice that lack DNA polymerase λ

(Kobayashi et al., 2002) or HFH4 (Chen et al., 1998; Brody et al., 2000).

The *Inv* (*Invs* – Mouse Genome Informatics) mutation is unique in that homozygous mutant mice exhibit LR reversal instead of LR randomization (Yokoyama et al., 1993). Unexpectedly, nodal flow in the *Inv* mutant embryo was shown to be leftward, although it was slow and turbulent (Okada et al., 1999). It remains unclear how such a slow, turbulent flow might result in LR reversal, although plausible models have been proposed (Okada et al., 1999). The *Inv/Inv* mouse may thus be the only mutant whose defects in LR patterning cannot be simply explained by nodal flow. The *Inv* gene is expressed ubiquitously in developing mouse embryos and encodes a protein that contains ankyrin repeats and calmodulin-binding motifs (Mochizuki et al., 1998; Morgan et al., 1998). Overexpression of the mouse Inv protein in frog embryos perturbed LR decision making (Yasuhiko et al., 2001), but the precise functions of this protein remain unclear.

We have now generated transgenic mice that express a fusion construct of Inv and green fluorescent protein (Inv::GFP). Our observations of the subcellular localization of this fusion protein suggest that Inv contributes to LR determination as a component of monocilia in the node.

MATERIALS AND METHODS

Generation of *Inv::GFP* transgenic mice

The coding region of the mouse *Inv* cDNA was linked to the 5′ end of the coding sequence for enhanced GFP derived from pEGFP N3 (Clontech). The *Inv::GFP* fusion cDNA was subcloned into a BOS EX vector (Mizushima and Nagata, 1990) (kindly provided by S. Nagata) under the control of the elongation factor 1α (EF1α) gene promoter, to yield *BOS-Inv::GFP* and to ensure that the fusion gene was expressed ubiquitously and robustly. The *InvΔC::GFP* construct was generated by deleting the 3′ part of the coding region of the *Inv* cDNA at the *Nhe*I site. Transgenic mice were generated by pronuclear injection of DNA into fertilized eggs obtained from the mating of *inv/+* FVB mice (Saijoh et al., 1999). Crossing of *Inv/+, Inv::GFP* mice with *Inv/+* mice yielded *Inv/Inv, Inv::GFP* animals. The presence of the transgene was verified by Southern blot analysis with the GFP coding sequence as a probe. GFP fluorescence in newborn mice was observed with a stereomicroscope (Leica MZ FLIII). For *Inv::GFP*, ten lines of transgenic mice were initially obtained. Eight of them expressed Inv::GFP and their transgenes were able to rescue the *situs* defects and polycystic kidney of the *Inv/Inv*mouse. In the remaining two lines, the transgene failed to rescue these *Inv/Inv* defects. For *InvΔC::GFP*, four transgenic mice were established. In three of them, the transgene could rescue situs defects but not polycystic kidney of the *Inv/Inv* mouse. Among these transgenic lines produced, those expressing the transgenes at a relatively high level, B27 (*Inv::GFP*) and N105 (*InvΔC::GFP*), were mainly used in this study. Founder mice for the B27 and N105 lines were *Inv/+* and +/+, respectively.

Preparation of antibodies to Inv

A 0.6 kb *Pvu*II fragment of the mouse *Inv* cDNA corresponding to the region of Inv located downstream of the ankyrin repeats was subcloned into the pGEX-4T vector (Pharmacia). The encoded glutathione S-transferase (GST)-Inv fusion protein was expressed in *Escherichia coli* strain AD202 (Akiyama and Ito, 1990), purified by chromatography on glutathione-Sepharose 4B (Pharmacia), and injected into rabbits. Polyclonal antibodies specific for Inv were isolated by preabsorption of rabbit serum with GST followed by affinity purification.

Generation of primary fibroblasts and cell culture

Primary fibroblasts expressing the Inv::GFP fusion protein were established from the skin of newborn transgenic animals. The cells were cultured in plastic dishes with Dulbecco's modified Eagle's medium supplemented with 10% fetal bovine serum and antibiotics. For immunofluorescence staining, the cells were cultured on cover slips for several days, fixed with 2% paraformaldehyde and stained with specific antibodies as described below.

Western blot analysis

Primary fibroblast cells were lysed in cell lysis buffer containing 20 mM Tris Hcl, 1% TritonX-100, 0.25% Deoxicorate, 250 mM NaCl, 5 mM EDTA, 1 mM PMSF. The lysates containing 20 μg protein were loaded on 10% SDS-polyacrylamide gels. An affinity-purified polyclonal anti-Inv antibody and a horseradish peroxidase-conjugated goat anti-rabbit antibody (Jackson) were used as the primary and secondary antibodies, respectively. Immune complexes were detected with ECL Western blot Detection Systems (Amersham).

Immunofluorescence analysis

Freshly isolated tissues were frozen in OCT compound (Tissue-Tec) and then cryosectioned (at 8 μm). After fixation with 2% paraformaldehyde, the sections were incubated with rabbit polyclonal antibodies to Inv, to GFP (MBL) or to calmodulin (Zymed), or with mouse monoclonal antibodies to acetylated tubulin (Sigma) or to γ-tubulin (Sigma). Antibodies were diluted in phosphate-buffered saline containing 5% skim milk and 0.05% Tween 20. All antibodies were diluted 1/1000 for staining sections, or 1/5000 for whole-mount staining. Immune complexes were detected with Alexa 488-conjugated goat antibodies to rabbit immunoglobulin G (Molecular Probes) or Alexa 568-conjugated goat antibodies to mouse immunoglobulin G (Molecular Probes). For whole-mount immunofluorescence analysis, freshly isolated embryos were fixed with ice-cold acetone and then incubated consecutively with primary and secondary antibodies at 4°C for 48 and 24 hours, respectively, in phosphate-buffered saline containing 5% skim milk and 1% Triton X-100. Confocal images were obtained with a Carl Zeiss confocal microscope (LSM 510) and three-dimensional images were reconstructed with the LSM 510 software (version 2.5).

Histological analysis

Kidneys were fixed in Bouin's solution, dehydrated and embedded in paraffin wax. Serial sections (5 μm) were prepared and stained with Hematoxylin and Eosin according to standard procedures.

RESULTS

A functionally active *GFP-Inv* transgene

To characterize the subcellular localization of the Inv protein, we generated transgenic mice that express an Inv::GFP fusion protein. The transgene, *BOS-Inv::GFP*, was designed to express a fusion protein in which the GFP sequence is fused in frame to the C terminus of Inv (Fig. 1A). The *Inv::GFP* construct was placed under the control of the promoter of the *Ef1a* (*Eif1a* – Mouse Genome Informatics) gene (Mizushima and Nagata, 1990), which confers ubiquitous and high-level expression. The *BOS-Inv::GFP* transgene was microinjected into mouse fertilized eggs (+/+ or *+/Inv*), resulting in the generation of several transgenic lines expressing Inv::GFP. Unless indicated otherwise, the B27 line, which expresses Inv::GFP at a relatively high level, was used in the present study. Mice harboring the *Inv::GFP* transgene (+/+ or *+/Inv*, *Inv::GFP*) were normal and fertile. Transgenic embryos expressed the fusion protein in a ubiquitous manner (Fig. 1B; data not shown), and newborn

transgenic mice were readily recognized by the presence of fluorescence in their limbs (Fig. 1C).

To determine whether the Inv::GFP protein is functional, we transferred the transgene to the *Inv/Inv* background. Homozygous *Inv* mutant mice exhibit situs inversus and die within a few weeks after birth as a result of polycystic kidney disease (Yokoyama et al., 1993). The laterality defects of *Inv/Inv* newborn mice are evident from the position of the stomach, which is located on the right side (Fig. 1D). The lung lobation pattern is also reversed, with one lobe on the right and four lobes on the left (Fig. 1E). The defects caused by the *Inv* mutation were rescued in *Inv/Inv* mice by expression of the *Inv::GFP* transgene. Thus, in *Inv/Inv, Inv::GFP* mice, the stomach was located on the left (Fig. 1D) and lung lobation was normal (one lobe on the left, four lobes on the right) (Fig. 1E). Moreover, *Inv/Inv, Inv::GFP* mice grew normally and were fertile, and they did not develop the polycystic kidney disease and jaundice characteristic of *Inv/Inv* animals (Fig. 1F,G). These observations thus indicated that the Inv::GFP protein is fully functional.

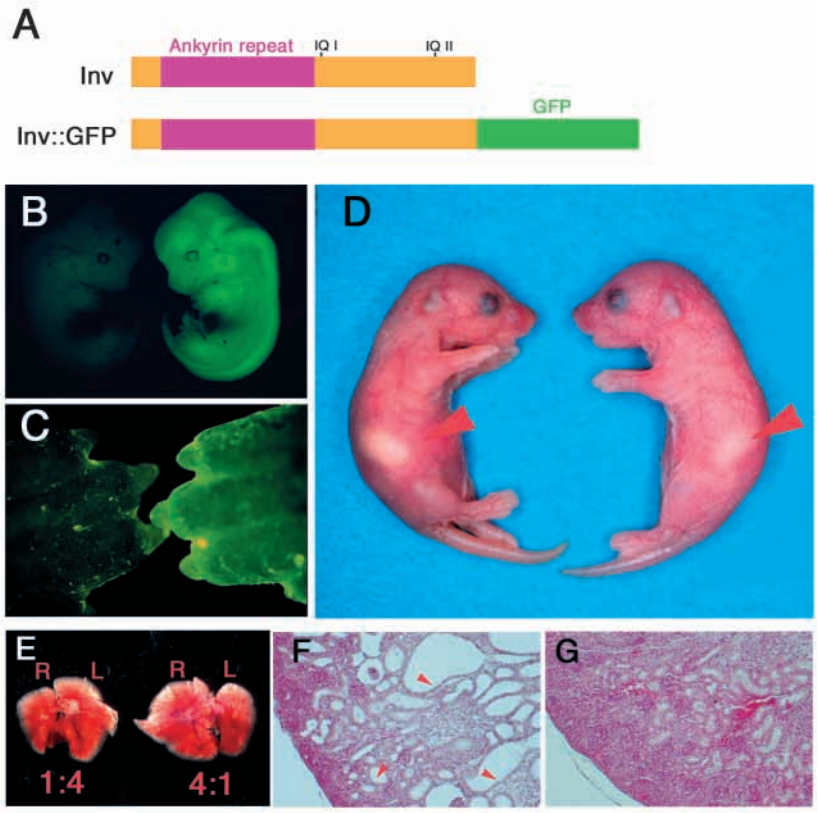

Fig. 1. Rescue of the *Inv/Inv* phenotype by expression of an *Inv::GFP* transgene. (A) Schematic representation of the structure of the Inv::GFP fusion protein. IQI and IQII represent two putative calmodulin binding motifs present in Inv. (B) Expression of the Inv::GFP fusion protein in a mouse embryo at embryonic day (E) 12.5. GFP fluorescence was detected in the transgenic embryo shown on the right but not in the non-transgenic littermate shown on the left. (C-G) Comparison of *Inv/Inv* mice with or without the *Inv::GFP* transgene at postnatal day 2. (C) Fluorescence was detected in the forelimb of an *Inv/Inv, Inv::GFP* mouse (right) but not in that of an *Inv/Inv* mouse without the transgene (left). (D) The stomach (arrowhead) was located on the right side of an *Inv/Inv* mouse (left embryo) but on the left side of an *Inv/Inv, Inv::GFP* mouse (right embryo). (E) Lung lobation pattern of an *Inv/Inv* mouse (left) and an *Inv/Inv, Inv::GFP* mouse (right). L, left; R, right. (F,G) The kidneys of an *Inv/Inv* mouse (F) exhibited multiple cysts (arrowheads) that were not present in the *Inv/Inv, Inv::GFP* mouse (G). Kidney sections were stained with Hematoxylin and Eosin.

Localization of Inv::GFP to the primary cilia of fibroblasts

We examined the subcellular localization of Inv::GFP in primary fibroblasts established from newborn *Inv/Inv, Inv::GFP* mice. In nonfixed cells, GFP fluorescence was detected in rod-like structures protruding from the cell body (Fig. 2A-C). To determine whether these structures were primary cilia, we subjected fixed fibroblasts to immunofluorescence staining for acetylated tubulin, a marker of primary cilia and centrioles. The rod-like structures that were positive for GFP were indeed detected by antibodies to acetylated tubulin (Fig. 2D-I). These results thus indicated that, in primary fibroblasts, Inv::GFP is preferentially localized to primary cilia.

We also examined the localization of the endogenous Inv protein in primary fibroblasts derived from newborn wild-type (non-transgenic) mice, with an anti-Inv antibody. In Western blot analysis (Fig. 3A), the anti-Inv antibody detected an 116 kDa protein in +/+, and *Inv/+* fibroblasts but not in *Inv/Inv* fibroblasts. The same antibody detected the Inv::GFP fusion protein of 140 kDa in *Inv/Inv, Inv::GFP* fibroblasts. In immunohistological staining, the anti-Inv antibody detected primary cilia in +/+ and *Inv/Inv, Inv::GFP* fibroblasts but not those in *Inv/Inv* fibroblasts (Fig. 2J-L, Fig. 3B), confirming the specificity of this antibody. These results indicate that the native Inv protein is also localized to primary cilia. The subcellular localization of Inv::GFP thus appeared to be indistinguishable from that of the native Inv protein.

Double staining of subconfluent cultures of primary fibroblasts derived from *Inv/Inv, Inv::GFP* mice with antibodies to GFP and antibodies to γ-tubulin revealed several distinct patterns of centriolar staining (Fig. 4A).

(1) Neither of the pair of centrioles was associated with a GFP signal (data not shown).

(2) One of the pair of centrioles was associated with a spot-like GFP signal (Fig. 4B).

(3) One of the pair of centrioles was associated with a rod-like GFP signal (Fig. 4C).

(4) One of the pair of centrioles was associated with an extended rod-like GFP signal (Fig. 4D).

Time-lapse observations revealed that these different staining patterns represent a temporal sequence from (1) to (4) during the formation of primary cilia (see Movie 1 at http://dev.biologists.org/supplemental/). Thus, the Inv::GFP signal first appeared associated with a mother centriole as it began to form a primary cilium; the fusion protein signal then elongated as the cilium extended from the older centriole, which becomes the basal body (extension of the Inv::GFP signal over a distance of 5 μm required ~ 50 minutes).

Localization of Inv::GFP to monocilia of the node

Given that the monocilia on the node pit cells are implicated in LR determination (Nonaka et al., 1998), we next examined the localization of Inv::GFP in the node. Observation of the node of *Inv/Inv, Inv::GFP* embryos from the ventral side without fixation (Fig. 5A) revealed a dot-like pattern of GFP fluorescence signals within the node (Fig. 5B). Lateral observation of the node revealed rod-shaped fluorescence signals protruding from the ventral node cells into the node cavity (Fig. 5C). Examination of the cells on the ventral side of the node at high magnification showed that Inv::GFP was present within the monocilia of these cells (Fig. 5D). The fusion protein was detected uniformly along the entire length of all the monocilia. Immunohistological analysis confirmed the preferential localization of Inv::GFP to monocilia of the ventral node cells. Monocilia that were detected with antibodies to acetylated tubulin (Fig. 5E) were thus also stained with antibodies to GFP (Fig. 5F). Together, these results demonstrated the preferential localization of Inv protein in node monocilia.

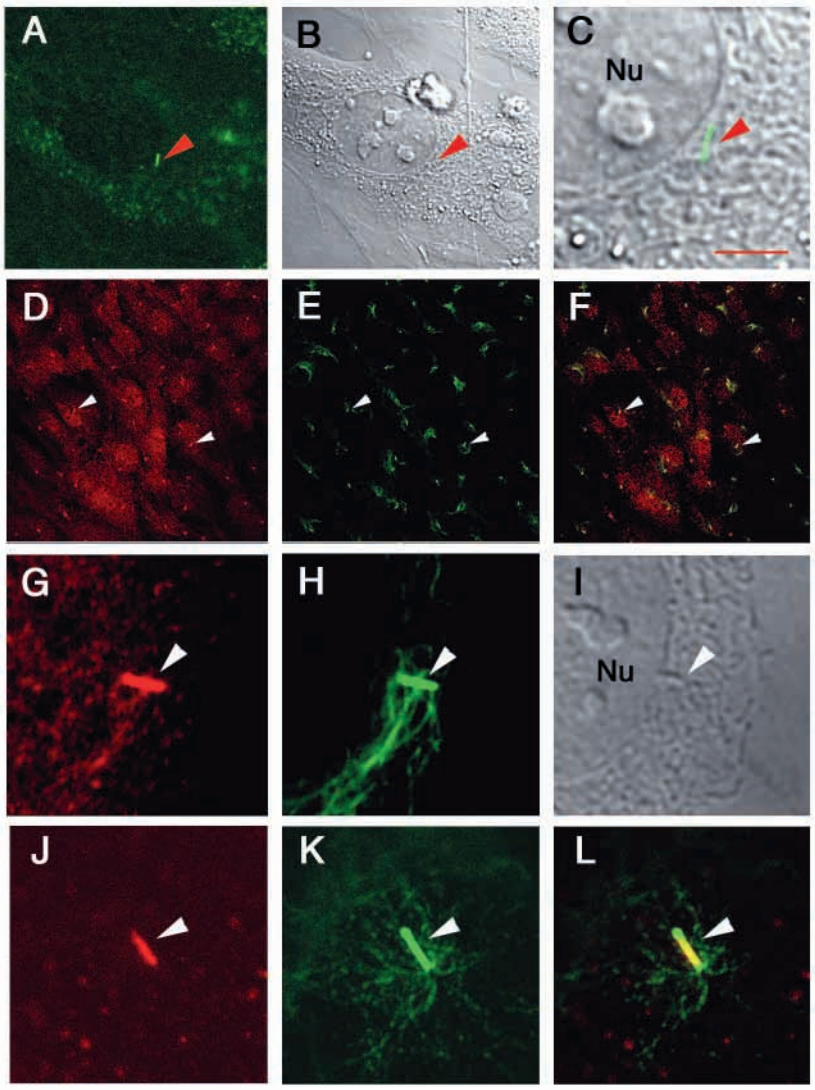

Fig. 2. Specific localization of GFP::Inv in the primary cilia of cultured fibroblasts. The subcellular localization of Inv was examined in primary fibroblasts established from *Inv/Inv, Inv::GFP* transgenic mice (A-I) or from wild-type (non-transgenic) mice (J-L). (A-C) Nonfixed cells were examined for GFP fluorescence (A) and by differential interference contrast (DIC) microscopy (B); the merged image of A and B is shown at higher magnification in C. GFP fluorescence was associated with rod-like structures (arrowheads) at the periphery of the nucleus (Nu). Scale bar: 5 μm. (D-I) Cells were fixed and subjected to double immunofluorescence staining with antibodies to GFP (red; D,G) and antibodies to acetylated tubulin (green; E,H). (F) Merged image of D,E. (G,H) Higher magnification views of D,E, respectively. (I) DIC image corresponding to G,H. The Inv::GFP fusion protein was specifically localized to primary cilia that were positive for acetylated tubulin (arrowheads). (J-L) Double staining with antibodies to Inv (red, J) and antibodies to acetylated tubulin (green, K). (L) Merged image of J,K. The endogenous Inv protein was also detected in the primary cilia of wild-type fibroblasts (arrowheads).

Localization of GFP::Inv to 9+0 cilia but not to 9+2 cilia

The cilia on node pit cells are monocilia; that is, they exhibit the 9+0 organization of microtubules. The preferential localization of Inv::GFP in the node monocilia prompted us to examine other 9+0 cilia as well as 9+2 cilia in *Inv/Inv, Inv::GFP* mice. Epithelial cells of the kidney collecting tubules possess 9+0 cilia. Examination of the kidneys of *Inv/Inv, Inv::GFP* mice revealed the presence of Inv::GFP in most of the cilia on the epithelial cells of the renal tubules, which were also positive for acetylated tubulin (Fig. 6A-C). Inv::GFP was also detected in the 9+0 cilia of the pituitary gland (Fig. 6D-F) and retina (Fig. 6G,H).

By contrast, Inv::GFP was not preferentially detected in 9+2 cilia, which are abundant in the epithelial cells of the respiratory system, oviduct and ependyma. Thus, in the oviduct (Fig. 6J-L) and ependyma (data not shown) of *Inv/Inv, Inv::GFP* embryos, Inv::GFP was not preferentially expressed in the cilia, revealed by their content of acetylated tubulin, but was instead present predominantly in the cytoplasm. In the trachea, Inv::GFP was detected in basal bodies stained by antibodies to γ-tubulin but not in the cilia (Fig. 6M-R). These observations thus revealed that, in cells with 9+2 cilia, Inv::GFP localized either to the cytoplasm or to the basal body, but did not accumulate preferentially in the ciliary body.

Inv is expressed ubiquitously in developing mouse embryos (Mochizuki et al., 1998). Inv::GFP was also expressed widely in transgenic mice because the transgene was placed under the control of the *Ef1a* gene promoter. In those cells without cilia, Inv::GFP was detected predominantly in the cytoplasm (Fig. 6I), but was occasionally detected in nuclei of some cell types such as skeletal muscle cells (data not shown). At adult stage, the transgene expression was detected in many organs, including the brain, muscle and testis (data not shown).

The mouse Inv protein contains two potential calmodulin binding (IQ) motifs (Mochizuki et al., 1998; Morgan et al., 1998) and interacts with

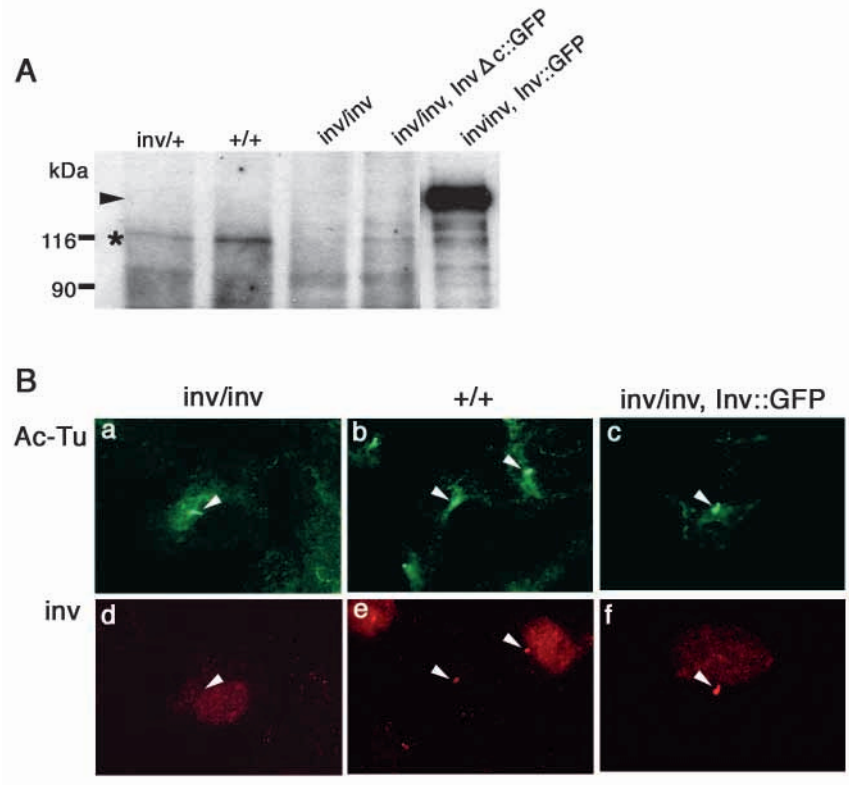

Fig. 3. The endogenous Inv protein is also localized to primary cilia. (A) Primary fibroblasts established from wild-type (+/+), *Inv/+*, *Inv/Inv*, *Inv/Inv, Inv::GFP* mice were subjected to western blot with an anti-Inv antibody. The endogenous Inv protein (asterisk) is detected in +/+ and *Inv/+* fibroblasts but not in *Inv/Inv* fibroblasts. The antibody also detected the Inv::GFP protein (arrowhead) in *Inv/Inv, Inv::GFP* fibroblasts. (B) Primary fibroblasts derived from *Inv/Inv*, +/+ or *Inv/Inv, Inv::GFP* mice were subjected to double staining with anti-acetylated tubulin (a-c, green) and anti-Inv antibody (d-f, red). Note that primary cilia are positive for acetylated tubulin (a-c, arrowheads). The anti-Inv antibody detects primary cilia in +/+ (e) and *Inv/Inv, Inv::GFP* (f) fibroblasts, but not those in *Inv/Inv* fibroblasts (d).

calmodulin in vitro (Yasuhiko et al., 2001; Morgan et al., 2002). Expression of the wild-type Inv protein in frog embryos perturbed LR determination, whereas expression of mutant Inv proteins that lack either of the two calmodulin binding motifs did not (Yasuhiko et al., 2001). These observations suggested that Inv may function through direct interaction with calmodulin. To test this hypothesis, we examined whether calmodulin colocalizes with Inv in cilia. Immunostaining of wild-type mouse embryo tissues with antibodies to calmodulin revealed the presence of this protein in 9+2 cilia, including those in the trachea (Fig. 7A-C), oviduct and ependyma (data not shown). By contrast, calmodulin was not detected in any of the 9+0 cilia examined, including those in the kidney (Fig. 7D-F), node (Fig. 7G-I), and pituitary gland (data not shown). Thus, whereas Inv is localized to 9+0 cilia, calmodulin is localized to 9+2 cilia.

Functional importance of the ankyrin repeat domain of Inv

The Inv protein also contains an ankyrin repeat domain, a motif that mediates protein-protein interaction. To investigate whether Inv might function by interacting with other proteins through its ankyrin repeats, we examined whether the N-terminal region of Inv including the ankyrin repeats was able to rescue the defects of *Inv/Inv* mice. We thus established permanent transgenic lines that express InvΔC::GFP, a chimeric protein in which the N-terminal region of Inv is fused to GFP (Fig. 8A). One of these lines (N105) that expressed InvΔC::GFP at a relatively high level was used for the studies described below. InvΔC::GFP protein appears to be unstable since the level of InvΔC::GFP protein detected in fibroblasts from *Inv/Inv; InvΔC::GFP* mice was always much lower than that of Inv::GFP in *Inv/Inv; Inv::GFP* fibloblasts (Fig. 3A).

The *InvΔC::GFP* transgene derived from N105 mice was transferred to the *Inv/Inv* background. Although *Inv/Inv, InvΔC::GFP* mice exhibited normal LR patterning of visceral organs, including the stomach and the lung, they developed polycystic kidney disease a few weeks after birth (Fig. 8B). The InvΔC::GFP protein was detected in the primary cilia of cultured fibroblasts derived from *Inv/Inv, InvΔC::GFP* mice as

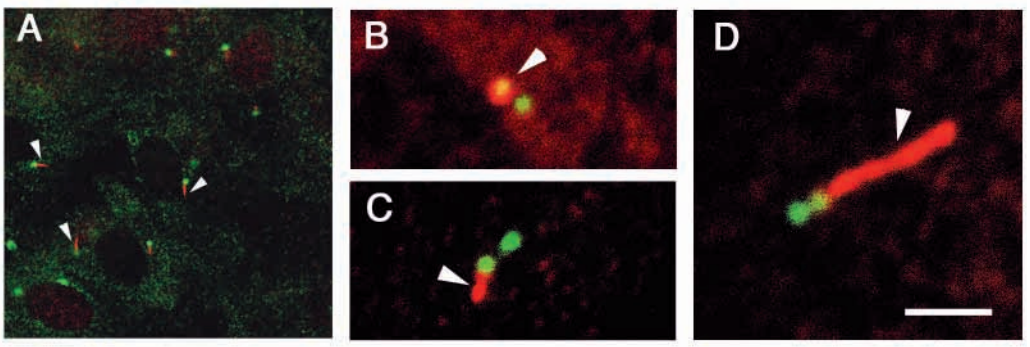

Fig. 4. Inv::GFP localization during cilium formation. Primary fibroblasts established from *Inv/Inv, Inv::GFP* transgenic mice were cultured until they were subconfluent and were then subjected to double staining with antibodies to GFP (red) and antibodies to γ-tubulin (green). A low-magnification view is shown in A and higher magnification views of centrosomal regions are shown in B-D. Several distinct patterns of Inv::GFP staining were detected. (B) Inv::GFP is localized to one of the centrioles, the mother centriole, even before extension of a cilium becomes obvious (arrowhead). (C) Inv::GFP is restricted to the extension of a mother centriole as it begins to form a cilium. (D) Inv::GFP is present along the entire length of a fully developed cilium. Scale bar: 2.5 μm.

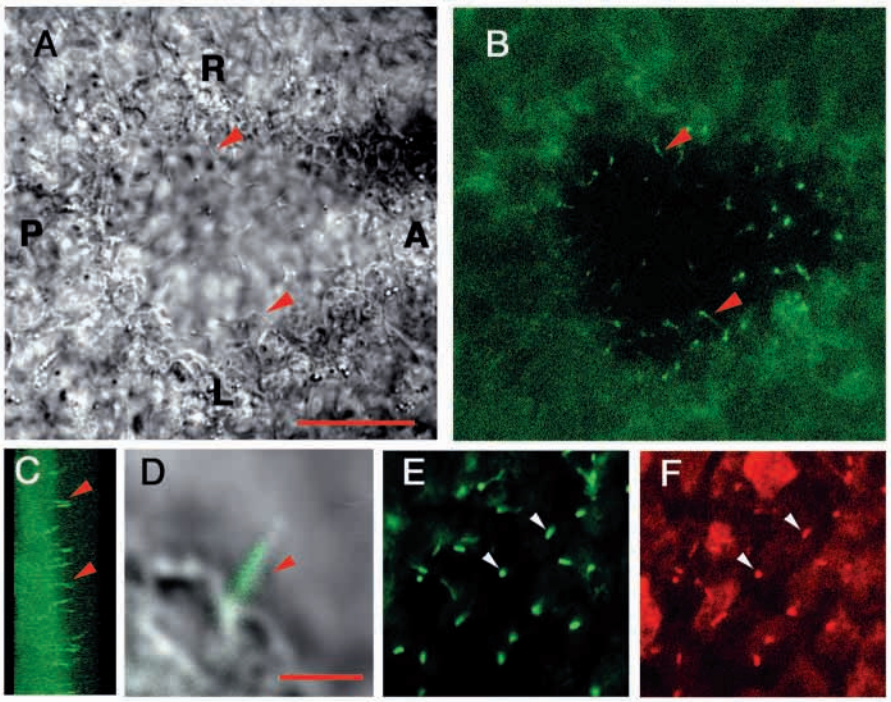

Fig. 5. Localization of Inv::GFP to the monocilia of the node. The node of *Inv/Inv, Inv::GFP* embryos at E8.0 was examined with a confocal microscope. The Inv::GFP fusion protein was preferentially localized to the cilia of the node (arrowheads). (A) DIC image of the ventral side of the node of a nonfixed embryo. (B) GFP fluorescence image of the node region shown in A. Many dots of fluorescence are apparent in the node. A, anterior; L, left; P, posterior; R, right. (C) Lateral view of the node reconstructed from serially *z*-scanned confocal images of GFP fluorescence. (D) Merged GFP fluorescence and DIC images of a single node cilium. (E,F) Double staining of an embryo with antibodies to acetylated tubulin (green; E) and antibodies to GFP (red; F). The node cilia, as revealed by their content of acetylated tubulin, were also positive for GFP. Scale bars: in A 20 μm for A,B; in D, 2.5 μm for D.

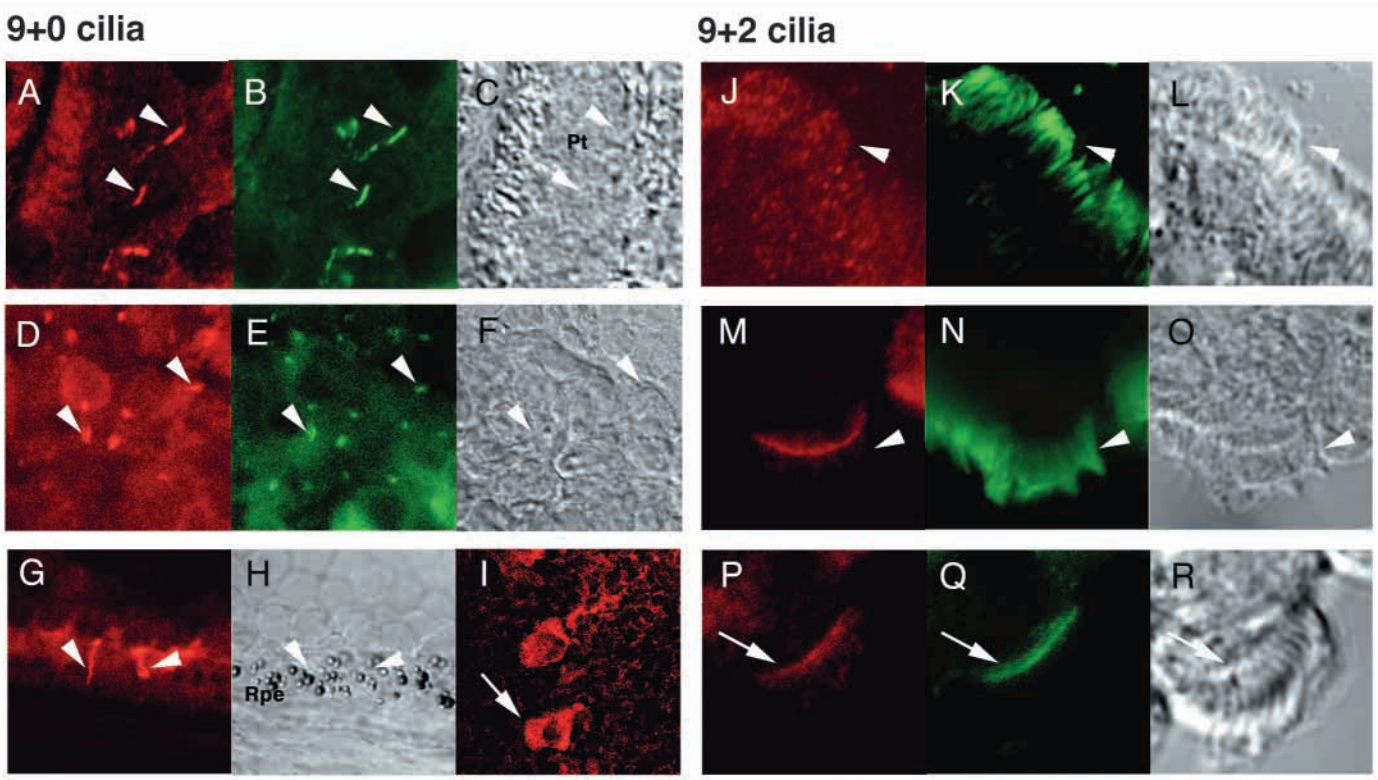

Fig. 6. Localization of Inv::GFP to 9+0 cilia but not to 9+2 cilia. Sections of the kidney (A-C), pituitary (D-F), retina (G,H), cerebellum (I), oviduct (J-L) and trachea (M-R) of *Inv/Inv, Inv::GFP* mice were subjected to double immunostaining with antibodies to GFP (red) (A,D,G,I,J,M) and antibodies to acetylated tubulin (green) (B,E,K,N) or with antibodies to GFP (red; P) and antibodies to γ-tubulin (green; Q). DIC images are shown at the right of corresponding fluorescence images (C,F,H,L,O,R). Note the prominent localization of Inv::GFP in 9+0 cilia (arrowheads) of kidney (A-C), pituitary gland (D-F) and retinal (G,H) cells. The fusion protein was not detected in the 9+2 cilia (arrowheads) of oviduct (J-L) or tracheal (M-O) cells, but was detected in the cytoplasm (arrow) of the Purkinje cells (I, arrow) and in the basal body (arrows) of tracheal cells (P-R, arrows). Both 9+0 and 9+2 cilia were positive for acetylated tubulin (B,E,K,N) and the basal body was positive for γ-tubulin (Q). Pt, proximal tubule; Rpe, retinal pigment epithelium.

well as in the monocilia of the node (Fig. 8C). It was not apparent, however, in the 9+0 cilia of the kidney (Fig. 8C), consistent with the failure of the transgene to rescue the kidney defect of *Inv/Inv* mice. These results thus suggest that InvΔC is able to localize to 9+0 cilia and to function as an LR determinant. The absence of InvΔC::GFP in the kidney is most probably due to the unstable nature of this protein.

Rescue of the laterality defects of *Inv/Inv* embryos by artificial nodal flow

The localization of the Inv::GFP protein in 9+0 cilia prompted us to examine the node monocilia of *Inv/Inv* embryos. Scanning electron microscopy revealed that the cilia of the *Inv/Inv* embryos were indistinguishable from those of wild-type embryos in their length, thickness and shape (data not shown). Video microscopy also revealed that the node cilia of *Inv/Inv* embryos rotate at a speed of 600 rpm in a clockwise direction, just like those of wild-type embryos. Thus, we were not able to detect any abnormalities of the node monocilia in *Inv/Inv* mice.

We recently developed an experimental system for the culture of mouse embryos under conditions of artificial flow of the culture medium (Nonaka et al., 2002). With this system, we showed that artificial nodal flow is able to determine LR patterning of wild-type embryos in a manner dependent on the direction and speed of flow and on the developmental stage of the embryo (Nonaka et al., 2002). We therefore tested whether artificial nodal flow was able to rescue the laterality defects of *Inv/Inv* mice. Exposure of *Inv/Inv* embryos to a fast leftward flow resulted in normal heart looping and normal embryonic turning (Fig. 9). This rescue of the LR patterning defects of *Inv/Inv* mice by artificial leftward flow suggested that nodal flow is impaired in *Inv/Inv* embryos. This conclusion is consistent with previous observations that nodal flow is slow and turbulent in *Inv/Inv* embryos (Okada et al., 1999), and it supports the idea that Inv plays a role in LR decision making as a component of the node monocilia.

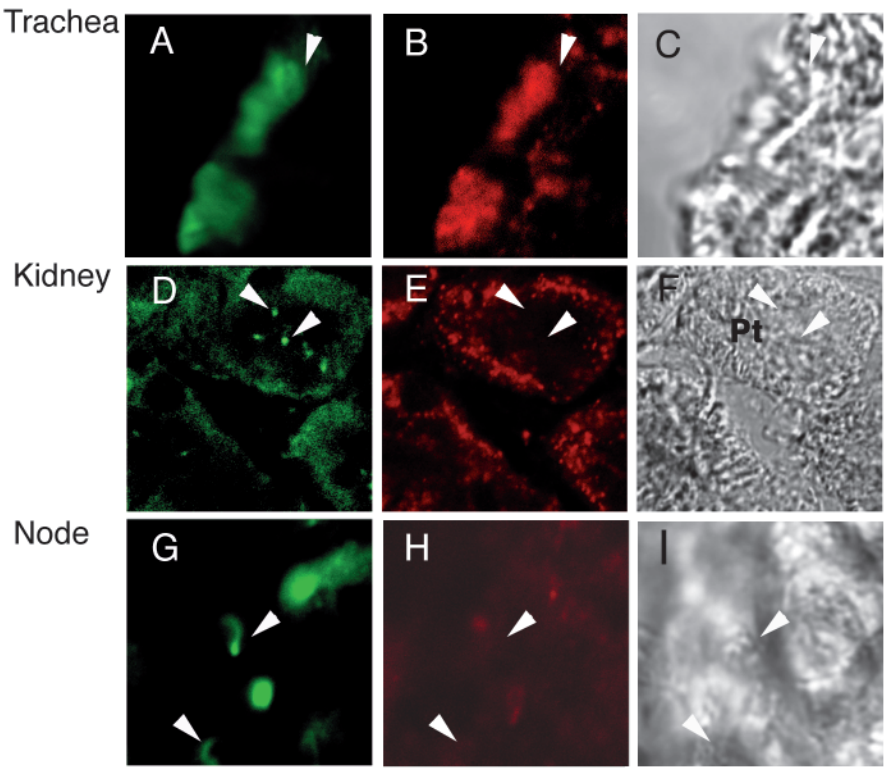

Fig. 7. Localization of calmodulin to 9+2 cilia. Sections both of the trachea (A-C) and kidney (D-F) of newborns and of the node (G-I) of embryos at E8.0 were subjected to double staining with antibodies to acetylated tubulin (green) (A,D,G) and antibodies to calmodulin (red) (B,E,H). Corresponding DIC images are shown on the right of each pair of fluorescence images (C,F,I). Calmodulin was localized to the 9+2 cilia (arrowheads) of tracheal cells, but not in the 9+0 cilia (arrowheads) of the kidney and node.

DISCUSSION

Preferential localization of Inv in 9+0 cilia

Our data indicate that Inv is preferentially localized to various 9+0 cilia (monocilia) but not to 9+2 cilia. A recent study (Nurnberger et al., 2002) reported the presence of Inv immunoreactivity in nuclei and at the cell membrane, but not in the primary cilia, of cultured Madin-Darby canine kidney (MDCK) cells, which resemble kidney epithelial cells. However, transfection of MDCK cells with pBOS-Inv::GFP revealed that the Inv::GFP protein was localized to the monocilia (data not shown). The reason for this apparent discrepancy is not clear. We also observed the nuclear localization of Inv::GFP in certain cell types, such as skeletal muscle cells, of transgenic mice, suggesting that the subcellular distribution of Inv may be dependent on cell type.

In mammals, primary cilia are present in a variety of organs at embryonic and adult stages. With a few exceptions, such as the role of node monocilia in LR patterning, the precise functions of these cilia remain unknown. Although node monocilia are motile (Sulik et al., 1994; Nonaka et al., 1998), most primary cilia are thought to be immotile. For example, monocilia present in the proximal tubule of the kidney are relatively long compared with the diameter of the collecting tube and coexist with numerous microvilli, making it unlikely that they are able to move actively. Such immotile primary cilia have been proposed to function as signal sensors, in which case Inv may be required not only for the movement of primary cilia (as in the node cilia) but also for the reception of external signals by these structures.

Role of Inv in LR determination

Substantial evidence implicates the node monocilia and nodal flow in LR determination. The localization of Inv to 9+0 monocilia further supports a role for node cilia in LR decision making. However, the mechanism by which nodal flow directs LR patterning is not known. As previously suggested (Nonaka et al., 1998), nodal flow may transport a molecule that acts as

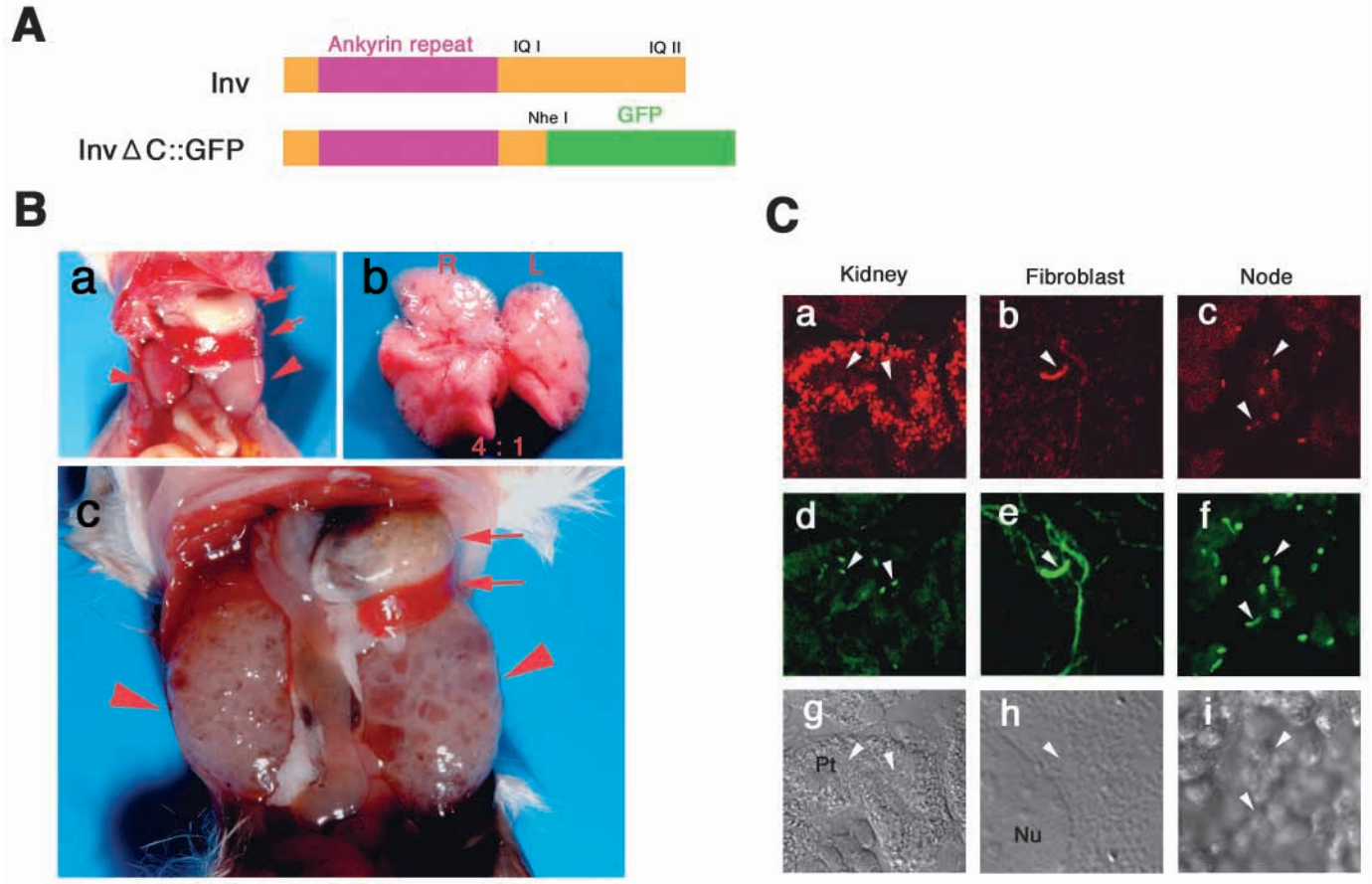

Fig. 8. Localization of the ankyrin repeat domain of Inv to the node cilia and its rescue of LR defects of *Inv/Inv* mice. (A) Schematic representation of the InvΔC::GFP fusion protein. (B) Phenotype of *Inv/Inv* mice harboring the *InvΔC::GFP* transgene at 2 weeks (a,b) or 4 weeks (c) of age. The transgene rescued the LR defects of *Inv/Inv* mice as revealed by the normal locations of the stomach and spleen (arrows in a,c) and the normal lobation pattern (L:R, 1:4) of the lungs (b). Although the kidneys appeared normal at 2 weeks (arrowheads in a), they were polycystic at 4 weeks (arrowheads in c). (C) Localization of the InvΔC::GFP protein in cells of *Inv/Inv, InvΔC::GFP* mice. Kidney sections of newborn animals, primary fibroblasts and E8.0 embryos were double immunostained with antibodies to GFP (red, a-c) and antibodies to acetylated tubulin (green, d-f), as indicated. The corresponding DIC images are shown below each pair of fluorescence images (g-i). InvΔC::GFP was detected in the primary cilia of cultured fibroblasts and in the monocilia of the embryonic node, but not in the 9+0 cilia of the kidney. Arrowheads indicate the positions of cilia.

a LR determinant toward the left side. Alternatively, the direction of or mechanical stress generated by the flow may be sensed differentially by cells on the two sides of the embryo. The Inv protein may thus be required for correct movement of the node cilia or for receiving signals generated by the flow. Our observations favor the former possibility but do not exclude the latter.

The mouse Inv protein possesses two calmodulin binding (IQ) motifs, both of which indeed bind calmodulin in vitro (Yasuhiko et al., 2001; Morgan et al., 2002). Whereas mouse Inv perturbed LR determination when ectopically expressed in *Xenopus* embryos, mutant Inv proteins lacking either of the two calmodulin binding motifs exhibited no such activity (Yasuhiko et al., 2001). These observations were thus suggestive of a functional interaction between Inv and the Ca^{2+}-binding protein calmodulin. However, our data do not support a role for such an interaction in LR patterning. First, we showed that these two proteins are not colocalized in the mouse embryo; rather, they show reciprocal expression patterns in that calmodulin is present in 9+2 cilia, whereas Inv is localized to 9+0 cilia. Second, in contrast to the observations made with frog embryos (Yasuhiko et al., 2001), the InvΔC::GFP protein, which lacks the C-terminal region (including one of the calmodulin binding motifs) of Inv, was able to rescue the LR defects of *Inv/Inv* mice. Nonetheless, it is formally possible that Inv interacts with low levels of calmodulin because the InvΔC::GFP protein retains the N-terminal calmodulin binding motif. Our data do not exclude a role for Ca^{2+} in Inv function, in which regard mice lacking polycystin 2, a putative Ca^{2+} channel, have been shown to exhibit LR defects (Pennekamp et al., 2002).

Artificial nodal flow was able to rescue the LR patterning defects of *Inv/Inv* mice. This result is consistent with previous observations that nodal flow of *Inv/Inv* embryos is leftward but slow and turbulent (Okada et al., 1999). Inv may thus be required for the correct movement of node cilia. Our examination of the node monocilia of *Inv/Inv* mice, however, failed to reveal any apparent anomalies in their morphology or motility. Further investigations of the fine structure and movement of the node monocilia in these mutant animals

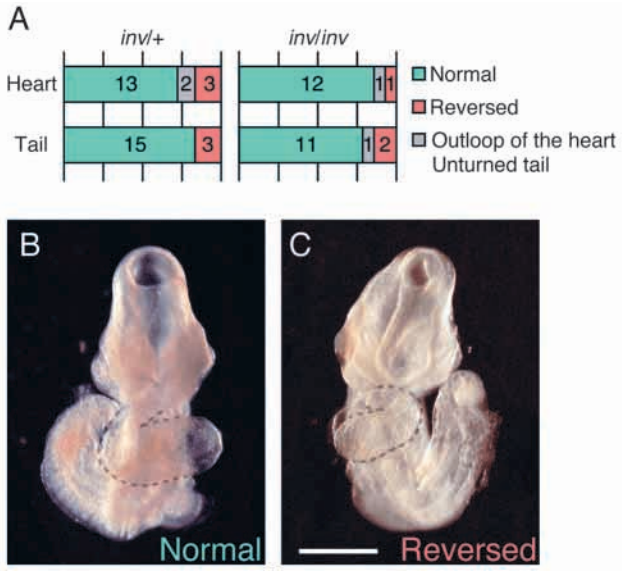

Fig. 9. Rescue of the LR defects of *Inv/Inv* embryos by artificial nodal flow. Both *Inv/+* and *Inv/Inv* embryos were exposed to artificial leftward flow as described previously (Nonaka et al., 2002) and were then examined for the directions of heart looping and embryonic turning. (A) The numbers of embryos that exhibited normal or reversed heart looping or embryonic turning, or outlooping of the heart or an unturned tail were determined. (B,C) Examples of the rescued (B) and non-rescued (C) *Inv/Inv* embryos are shown. Heart looping is indicated by the broken lines. Scale bar: 1 mm.

are thus required to detect possible abnormalities. The development of an imaging system that allows observation of the cilia of live mouse embryos at high magnification would facilitate this goal.

Node monocilia may also function as signal sensors. Our data with artificial nodal flow may not favor this notion, but they do not exclude the possibility that Inv plays dual roles in generating correct nodal flow and in transducing signals generated by such flow. Numerous examples of immotile cilia that function in sensory perception, including chemoreception, photoreception and mechanoreception, have been described in nonvertebrates. In *Caenorhabditis elegans*, cilia are present in 60 out of the 302 neurons, in which they function as sensory organelles (Bargmann and Horvitz, 1991; Dwyer et al., 1998). In *Chlamydomonas*, flagella transduce signals during gamete adhesion in mating (Solter and Gibor, 1977; Pan and Snell, 2002). Furthermore, in the mouse, the polaris protein is required for formation both of 9+0 cilia such as node monocilia (Murcia et al., 2000) and of 9+2 cilia such as those in brain ependymal cells. A polaris homolog in *C. elegans*, OSM-5, localizes to the basal body and cilia and functions in intraflagellar transport; in *osm-5* mutants, sensory neurons lack cilia that function as sensors of osmotic pressure (Haycraft et al., 2001; Taulman et al., 2001). Whether or not node cilia (and Inv) function in sensory perception remains to be determined.

Role of Inv in kidney development

Homozygous *Inv* mutant mice develop polycystic kidney disease a few weeks after birth. Furthermore, many of the genes required for LR determination, including *Inv*, polaris and polycystin 2, are also implicated in polycystic kidney disease in humans. In general, the histological features of polycystic kidneys are first apparent in the proximal collecting tubules. Our examination of eight independent *Inv/Inv, Inv::GFP* transgenic lines revealed that the abundance of Inv::GFP protein in monocilia of the proximal collecting tubules in newborns correlated with the severity of polycystic kidney disease at later stages (data not shown). This correlation, together with the localization of Inv::GFP in the monocilia of the kidney epithelium, suggests that Inv functions in these cilia. However, examination of the kidney monocilia of *Inv/Inv* newborn mice (before polycystic kidney disease becomes severe) revealed no apparent anomalies with respect to the number or morphology of the cilia (data not shown). Although the precise mechanism responsible for the development of polycystic kidney disease in *Inv/Inv* mice is unknown, the kidney monocilia may function as organelles that sense external signals, such as ion concentration, osmotic pressure or mechanical flow, and Inv may be required for transduction of such signals.

We thank Dr Tadanobu Ban for introducing us electron microscopy; and Kyoko Mochida and Sachiko Ohishi for technical assistance. This work was supported by CREST (Core Research for Evolutional Science and Technology) of the Japan Science and Technology Corporation.

REFERENCES

Akiyama, Y. and Ito, K. (1990). SecY protein, a membrane-embedded secretion factor of *E. coli*, is cleaved by the OmpT protease in vitro. *Biochem. Biophys. Res. Commun.* **167**, 711-715.

Bargmann, C. I. and Horvitz, H. R. (1991). Chemosensory neurons with overlapping functions direct chemotaxis to multiple chemicals in *C. elegans*. *Neuron* **7**, 729-742.

Beddington, R. S. and Robertson, E. J. (1999). Axis development and early asymmetry in mammals. *Cell* **96**, 195-209.

Brody, S. L., Yan, X. H., Wuerffel, M. K., Song, S. K. and Shapiro, S. D. (2000). Ciliogenesis and left-right axis defects in forkhead factor HFH-4-null mice. *Am. J. Respir. Cell Mol. Biol.* **23**, 45-51.

Brown, N. A., McCarthy, A. and Wolpert, L. (1991). Development of handed body asymmetry in mammals. *Ciba Found. Symp.* **162**, 182-196.

Brown, N. A. and Wolpert, L. (1990). The development of handedness in left/right asymmetry. *Development* **109**, 1-9.

Capdevila, J., Vogan, K. J., Tabin, C. J. and Izpisua Belmonte, J. C. (2000). Mechanisms of left-right determination in vertebrates. *Cell* **101**, 9-21.

Chen, J., Knowles, H. J., Hebert, J. L. and Hackett, B. P. (1998). Mutation of the mouse hepatocyte nuclear factor/forkhead homologue 4 gene results in an absence of cilia and random left-right asymmetry. *J. Clin. Invest.* **102**, 1077-1082.

Dwyer, N. D., Troemel, E. R., Sengupta, P. and Bargmann, C. I. (1998). Odorant receptor localization to olfactory cilia is mediated by ODR-4, a novel membrane-associated protein. *Cell* **93**, 455-466.

Fujinaga, M. (1997). Development of sidedness of asymmetric body structures in vertebrates. *Int. J. Dev. Biol.* **41**, 153-186.

Hamada, H., Meno, C., Watanabe, D. and Saijoh, Y. (2002). Establishment of vertebrate left-right asymmetry. *Nat. Rev. Genet.* **3**, 103-113.

Haycraft, C. J., Swoboda, P., Taulman, P. D., Thomas, J. H. and Yoder, B. K. (2001). The *C. elegans* homolog of the murine cystic kidney disease gene *Tg737* functions in a ciliogenic pathway and is disrupted in *osm-5* mutant worms. *Development* **128**, 1493-1505.

Kobayashi, Y., Watanabe, M., Okada, Y., Sawa, H., Takai, H., Nakanishi, M., Kawase, Y., Suzuki, H., Nagashima, K., Ikeda, K. and Motoyama, N. (2002). Hydrocephalus, situs inversus, chronic sinusitis and male infertility in DNA polymerase lambda-deficient mice: possible implication for the pathogenesis of immotile cilia syndrome. *Mol. Cell. Biol.* **22**, 2769-2776.

Marszalek, J. R., Ruiz-Lozano, P., Roberts, E., Chien, K. R. and Goldstein, L. S. (1999). Situs inversus and embryonic ciliary morphogenesis defects in

mouse mutants lacking the KIF3A subunit of kinesin-II. *Proc. Natl. Acad. Sci. USA* **96**, 5043-5048.

Mizushima, S. and Nagata, S. (1990). pEF-BOS, a powerful mammalian expression vector. *Nucleic Acids Res.* **18**, 5322.

Mochizuki, T., Saijoh, Y., Tsuchiya, K., Shirayoshi, Y., Takai, S., Taya, C., Yonekawa, H., Yamada, K., Nihei, H., Nakatsuji, N., Overbeek, P. A., Hamada, H. and Yokoyama, T. (1998). Cloning of *inv*, a gene that controls left/right asymmetry and kidney development. *Nature* **395**, 177-181.

Morgan, D., Turnpenny, L., Goodship, J., Dai, W., Majumder, K., Matthews, L., Gardner, A., Schuster, G., Vien, L., Harrison, W. et al. (1998). *Inversin*, a novel gene in the vertebrate left-right axis pathway, is partially deleted in the *inv* mouse *Nature Genet.* **20**, 149-156.

Morgan, D., Goodship, J., Essner, J. J., Vogan, K. J., Turnpenny, L., Yost, J., Tabin, C. J. and Strachan, T. (2002). The left-right determinant inversin has highly conserved ankyrin repeat and IQ domains and interacts with calmodulin. *Hum. Genet.* **110**, 377-384.

Murcia, N. S., Richards, W. G., Yoder, B. K., Mucenski, M. L., Dunlap, J. R. and Woychik, R. P. (2000). The oak ridge polycystic kidney (ORPK) disease gene is required for left-right axis determination. *Development* **127**, 2347-2355.

Nonaka, S., Shiratori, H., Saijoh, Y. and Hamada, H. (2002). Determination of left-right patterning of the mouse embryo by artificial nodal flow. *Nature* **418**, 96-99.

Nonaka, S., Tanaka, Y., Okada, Y., Takeda, S., Harada, A., Kanai, Y., Kido, M. and Hirokawa, N. (1998). Randomization of left-right asymmetry due to loss of nodal cilia generating leftward flow of extraembryonic fluid in mice lacking KIF3B motor protein *Cell* **95**, 829-837.

Nurnberger, J., Bacallao, R. L. and Phillips, C. L. (2002). Inversin forms a complex with catenins and N-cadherin in polarized epithelial cells. *Mol. Biol. Cell* **13**, 3096-3106.

Okada, Y., Nonaka, S., Tanaka, Y., Saijoh, Y., Hamada, H. and Hirokawa, N. (1999). Abnormal nodal flow precedes situs inversus in *iv* and *inv* mice. *Mol. Cell* **4**, 459-468.

Pan, J. and Snell, W. J. (2002). Kinesin-II is required for flagellar sensory transduction during fertilization in *Chlamydomonas*. *Mol. Biol. Cell* **13**, 1417-1426.

Pennekamp, P., Karcher, C., Fischer, A., Schweickert, A., Skryabin, B., Horst, J., Blum, M. and Dworniczak, B. (2002). The ion channel polycystin-2 is required for left-right axis determination in mice. *Curr. Biol.* **12**, 938-943.

Saijoh, Y., Adachi, H., Mochida, K., Ohishi, S., Hirao, A. and Hamada, H. (1999). Distinct transcriptional regulatory mechanisms underlie left-right asymmetric expression of *lefty-1* and *lefty-2*. *Genes Dev.* **13**, 259-269.

Solter, K. M. and Gibor, A. (1977). Evidence for a role of flagella as sensory transducers in mating of *Chlamydomonas reinhardi*. *Nature* **265**, 444-445.

Sulik, K., Dehart, D. B., Iangaki, T., Carson, J. L., Vrablic, T., Gesteland, K. and Schoenwolf, G. C. (1994). Morphogenesis of the murine node and notochordal plate. *Dev. Dyn.* **201**, 260-278.

Supp, D. M., Witte, D. P., Potter, S. S. and Brueckner, M. (1997). Mutation of an axonemal dynein affects left-right asymmetry in inversus viscerum mice. *Nature* **389**, 963-966.

Supp, D. M., Brueckner, M., Kuehn, M. R., Witte, D. P., Lowe, L. A., McGrath, J., Corrales, J. and Potter, S. S. (1999). Targeted deletion of the ATP binding domain of left-right dynein confirms its role in specifying development of left-right asymmetries. *Development* **126**, 5495-5504.

Takeda, S., Yonekawa, Y., Tanaka, Y., Okada, Y., Nonaka, S. and Hirokawa, N. (1999). Left-right asymmetry and kinesin superfamily protein KIF3A: new insights in determination of laterality and mesoderm induction by *kif3A*$^{-/-}$ mice analysis. *J. Cell Biol.* **145**, 825-836.

Taulman, P. D., Haycraft, C. J., Balkovetz, D. F. and Yoder, B. K. (2001). Polaris, a protein involved in left-right axis patterning, localizes to basal bodies and cilia. *Mol. Biol. Cell* **12**, 589-599.

Wright, C. V. (2001). Mechanisms of left-right asymmetry: What's right and what's left? *Dev. Cell* **1**, 179-186.

Yasuhiko, Y., Imai, F., Ookubo, K., Takakuwa, Y., Shiokawa, K. and Yokoyama, T. (2001). Calmodulin binds to Inv protein: implication for the regulation of Inv function. *Dev. Growth Differ.* **43**, 671-681.

Yokoyama, T., Copeland, N. G., Jenkins, N. A., Montgomery, C. A., Elder, F. F. and Overbeek, P. A. (1993). Reversal of left-right asymmetry: a situs inversus mutation. *Science* **260**, 679-682.

Yost, H. J. (2001). Establishment of left-right asymmetry. *Int. Rev. Cytol.* **203**, 357-381.